

Theoretical study on the finite temperature magnetism of rare earth permanent magnets

A. Sakuma¹, D. Miura¹, R. Sasaki¹, and Y. Toga²

(¹ Department of Applied Physics, Tohoku University, Sendai 980-8579, Japan;

² National Institute for Materials Science (NIMS), Tsukuba 305-0047, Japan)

1. Introduction

From an industrial viewpoint, magnetic anisotropy is the most important property of ferromagnetic materials. It governs the efficiency of magnetic media in hard disk drive (HDD) devices, permanent magnets in motors and so on. Permanent magnets have strong magnetic anisotropy above room temperature, especially in motors of hybrid and electric vehicles. They are consequently highly desired in terms of addressing energy problem.

In this symposium, we will first overview the general theory for the magnetic anisotropy at finite temperature and show how the magnetic anisotropy constants (MAC) vary as temperature increases.^① Next, we will discuss on the effects of thermal fluctuation (activation) of magnetization on the reversal (coercive) field, on the basis of magnetic viscosity. Finally, let us show some calculated results for the temperature dependence of MAC of Nd₂Fe₁₄B and mainly discuss the site dependence of the MAC's at around the room temperature.^{②,③}

2. Theoretical evaluation of the magnetic anisotropy constants at finite temperature

Suppose that the classical Hamiltonian of a magnetic system having the uniaxial anisotropy is given by

$$H = \kappa_1 \sum_i \sin^2 \theta_i + \kappa_2 \sum_i \sin^4 \theta_i + H_{ex} \quad (1)$$

where the first two terms indicate the magnetic anisotropy energy and the last term the exchange energy. Here the constants κ_1 and κ_2 can be expressed through the expansion coefficients of the crystal field energy in terms of the Legendre polynomials $P_l(\cos \theta)$, from which we have $\kappa_1 = -3B_2^0 - 40B_4^0$ and $\kappa_2 = 35B_4^0$ with B_n^0 being the crystal field parameter. The methods to evaluate the temperature dependence of the MAC's are listed as follows:

- 1) to solve the stochastic LLG (Langevin) equation involving the thermally fluctuated field, and derive the MAC's by the magnetization curves for the applied fields parallel and perpendicular to the easy axis.
- 2) to calculate the free energy $F(\Theta, T)$ by performing the Monte-Carlo method with the average magnetization direction of Θ , and derive the n-th MAC's $K_n(T)$ by fitting $F(\Theta, T)$ with $K_1(T)\sin^2 \Theta + K_2(T)\sin^4 \Theta$.
- 3) to express directly the form of MAC's by means of the first order perturbation theory in terms of the anisotropy terms, which gives

$$K_1(T) = c_2 \kappa_1 + (8/7)(c_2 - c_4) \kappa_2, \quad K_2(T) = c_4 \kappa_2, \quad (2)$$

$$c_2 \equiv (1/2)\langle 3\cos^2 \theta - 1 \rangle_{H_{ex}} = \langle P_2(\cos \theta) \rangle_{H_{ex}}. \quad (3a)$$

$$c_4 \equiv (1/8)\langle 35\cos^4 \theta - 30\cos^2 \theta + 3 \rangle_{H_{ex}} = \langle P_4(\cos \theta) \rangle_{H_{ex}} \quad (3b)$$

Note that $K_1(0) = \kappa_1$ and $K_2(0) = \kappa_2$, since $c_l = 1$ when $T=0$.

Although the method 1) requires much computational time and resource, it is most realistic to reproduce the magnetization curves. To perform the method 2), it is useful to adopt a new technique proposed recently by Asselin et al.^④ Employing this method, we have successfully

reproduced the temperature dependence of MCA's of $\text{Nd}_2\text{Fe}_{14}\text{B}$.³⁾ The method 3) provides us physically transparent form of the MAC's and is the most convenient way to realize the MAC's if one further adopts the mean field approximation for the exchange term. One can understand from eqs. (2) and (3) that $K_1(T)$ ($T > 0$) is determined by κ_1 and κ_2 , and further by H_{ex} through $\langle P_l(\cos \theta) \rangle_{H_{ex}}$. Additionally, according to the Callen-Callen theory,⁵⁾ one should note the relation $\langle P_l(\cos \theta) \rangle_{H_{ex}} \approx \langle \cos \theta \rangle_{H_{ex}}^{l(l+1)/2} = \langle m \rangle_{H_{ex}}^{l(l+1)/2}$ where $\langle m \rangle_{H_{ex}} = M(T)/M(0)$. Recently, we have confirmed by using the methods 2) and 3) that the approximate relation $\langle P_l(\cos \theta) \rangle_{H_{ex}} \approx \langle m \rangle_{H_{ex}}^{l(l+1)/2}$ holds in the wide range of temperature as far as $k_B T < H_{ex}$ is satisfied. Thus, the MAC's can be expressed by using $\langle m \rangle_{H_{ex}} = M(T)/M(0)$ as $K_1(T) = (\kappa_1 + 8/7\kappa_2)\langle m \rangle_{H_{ex}}^3 - 8/7\kappa_2\langle m \rangle_{H_{ex}}^{10}$ and $K_2(T) = \kappa_2\langle m \rangle_{H_{ex}}^{10}$. In Fig. 1, we show the calculated results of the temperature dependence of MAC's of $\text{Nd}_2\text{Fe}_{14}\text{B}$ based on the above expressions. Here, we input the experimental data of $\langle m \rangle_{H_{ex}} = M(T)/M(0)$ and took into account for $\sin^6 \theta_i$ term in addition to κ_1 and κ_2 terms. One can recognize that the above expressions can work well for the complex compounds like $\text{Nd}_2\text{Fe}_{14}\text{B}$.

In addition, we should emphasize here that $K_n(T)$ ($T > 0$) is dominated by H_{ex} as well as κ_1 and κ_2 , as mentioned above. This implies that the $K_n(T)$ at surfaces or interfaces exhibit larger decrement with temperature than those inside the bulk. Figure 2 shows the temperature dependence of $K_1(T)$ both for $H_{ex} = 350$ and 175 in units of kelvin.¹⁾ One can see that the $K_1(T)$ values for $H_{ex} = 175$ [K] is much smaller than those for $H_{ex} = 350$ [K] as bulk values, when the temperature is above 200 [K], which leads us to consider that the magnetization reversal takes place by a smaller field at the surfaces or interfaces of grains in magnets.

In the symposium, we will discuss the site dependence of the MAE and the effects of thermal activation on the reversal field in Nd-Fe-Bd.

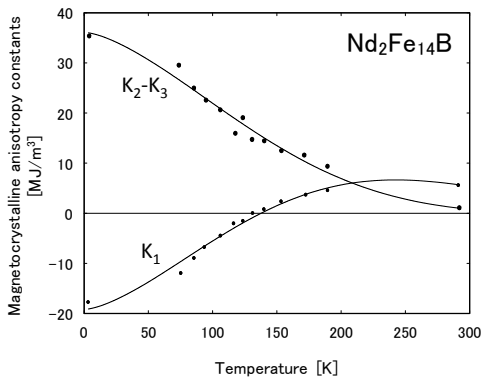


Fig. 1 Temperature dependence of K_1 and $K_2 - K_3$ of $\text{Nd}_2\text{Fe}_{14}\text{B}$. The dots are the experimental data.⁶⁾

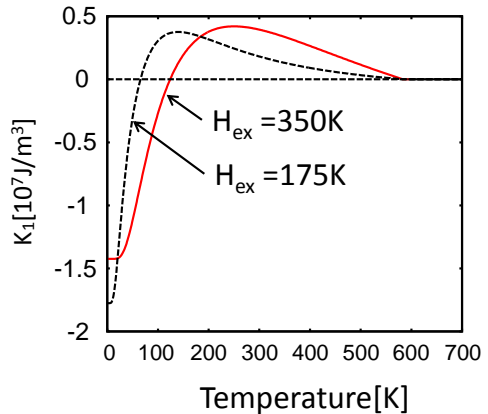


Fig. 2 Temperature dependence of K_1 for the exchange energy $H_{ex}=350$ and 175 [in units of K] in $\text{Nd}_2\text{Fe}_{14}\text{B}$.

References

- 1) D. Miura, R. Sasaki, and A. Sakuma, Applied Physics Express, **8**, 113003 (2015).
- 2) R. Sasaki, D. Miura, and A. Sakuma, Applied Physics Express, **8**, 043004 (2015).
- 3) Y. Toga, M. Matsumoto, S. Miyashita, H. Akai, S. Doi, T. Miyake, and A. Sakuma, to be submitted.
- 4) P. Asselin, et al., Phys. Rev. B **82**, 054415 (2010).
- 5) E. R. Callen and E. Callen, Phys. Rev. **129**, 578 (1966).
- 6) O. Yamada, et al., J. Magn. Magn. Mater. **54-57**, 585 (1986).

Monte Carlo analysis for finite temperature magnetism of $\text{Nd}_2\text{Fe}_{14}\text{B}$ magnet

Y. Toga^{A,F}, M. Matsumoto^{A,F}, S. Miyashita^{B,F}, H. Akai^{C,F}, S. Doi^{C,F}, T. Miyake^{D,F}, and A. Sakuma^E

^ANational Institute for Materials Science (NIMS), Tsukuba 305-0047, Japan

^BDepartment of Physics, The University of Tokyo, Bunkyo-Ku 113-0033, Japan

^CInstitute for Solid State Physics, The University of Tokyo, Kashiwa 277-8581, Japan

^DNational Institute of Advanced Industrial Science and Technology (AIST), Tsukuba 305-8568, Japan

^EDepartment of Applied Physics, Tohoku University, Sendai 980-8579, Japan

^FElements Strategy Initiative Center for Magnetic Materials (ESICMM), Japan

Rare earth permanent magnets, particularly Nd-Fe-B, exhibiting strong magnetic performance are attracting considerable attention because of the rapidly growing interest in electric vehicles. The main focus of research in involving these materials is to increase the coercive field H_c and improve the temperature dependence. Recently, Sasaki et al.¹⁾ conducted theoretical studies in the quantitative level on the temperature dependence of magnetic anisotropy for a $\text{Nd}_2\text{Fe}_{14}\text{B}$ bulk system. However, as these theories relied on the mean field approach, they are not enough to include the effects of magnetic inhomogeneities.

Because of the above background, we constructed a realistic classical three-dimensional Heisenberg model using results from first-principles calculations, and investigated the magnetic properties of the $\text{Nd}_2\text{Fe}_{14}\text{B}$ bulk system at finite temperatures. To analyze the finite-temperature magnetic anisotropy, we applied constrained Monte Carlo (C-MC) method²⁾ to the above classical Heisenberg model. The C-MC method fixes the direction of total magnetization, \mathbf{M} , in any direction for each MC sampling without external magnetic field. This allows us to calculate the angle θ dependencies of magnetization torque and free energy.

Figure 1 shows the y -direction torque and free energy as a function of magnetization angle θ . We can see that for 100K and 125K, the torque (free energy) curve attains a local maximum (minimum) at $\theta \neq 0$, which reflect the spin reorientation of $\text{Nd}_2\text{Fe}_{14}\text{B}$. In contrast, above $T \geq 200\text{ K}$, the local maximum (minimum) disappears and the torque (free energy) curve approaches $\propto \sin 2\theta$ ($\sin^2 \theta$). This behavior implies that the magnetic anisotropy constant K_1^A becomes dominant as the temperature increases.

We also discuss the external magnetic field H_{ext} response of the energy barrier (activation energy) which governs the probability of magnetization reversal via the thermal fluctuation of spins. Figure 2 shows the height of the energy barrier, \mathcal{F}_B , when H_{ext} is applied opposite to the z -direction of \mathbf{M} . The H_{ext} response of \mathcal{F}_B is generally expressed³⁾ by: $\mathcal{F}_B(H_{\text{ext}}) = \mathcal{F}_B^0(1 - H_{\text{ext}}/H_0)^n$. The exponent n can take various values, such as $n = 2$ for the Stoner-Wohlfarth model and $n = 1$ for the weak domain-wall pinning mechanism.³⁾ The parameters \mathcal{F}_B^0 , H_0 , and n were obtained by fitting $\mathcal{F}_B(H_{\text{ext}})$ in Fig. 2. We can find that n takes values of less than 2 in the low-temperature region (below the room temperature, $T_R \sim 300\text{ K}$) and approaches 2 as the temperature increases. This reflects the fact that the magnetic anisotropy is mainly governed by the K_1^A term in the high-temperature region.

- 1) R. Sasaki, D. Miura, and A. Sakuma, Appl. Phys. Express 8, 043004 (2015).
- 2) P. Asselin, R. F. L. Evans, J. Barker, R. W. Chantrell, R. Yanes, O. Chubykalo-Fesenko, D. Hinzke, and U. Nowak, Phys. Rev. B **82**, 054415 (2010).
- 3) P. Gaunt, J. Appl. Phys. **59**, 4129 (1986).

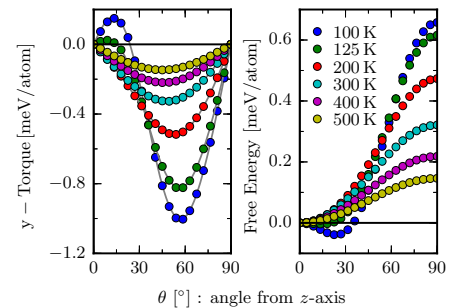


Fig. 1 Angular dependence of torque (left side) and free energy (right side) at each temperature.

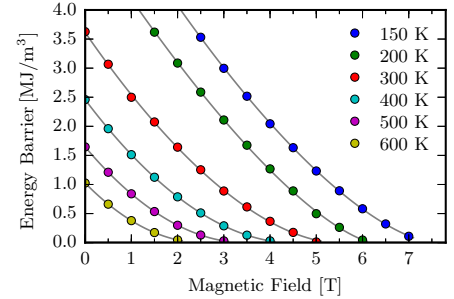


Fig. 2 Height of the energy barrier, \mathcal{F}_B , as a function of external magnetic field, H_{ext} , at each temperature.

希土類永久磁石化合物における交換結合制御による磁気異方性の耐熱性改善

松本宗久, 原嶋庸介*, 三宅隆*, 三俣千春
(物材機構, * 産総研)

Exchange-coupling engineering in rare-earth permanent-magnet compounds to improve the high-temperature magnetic anisotropy
M. Matsumoto, Y. Harashima*, T. Miyake*, and C. Mitsumata
(NIMS, * AIST)

1 はじめに

ハイブリッドカー・電気自動車の駆動部に使用される希土類永久磁石は摂氏マイナス40度から摂氏180度(絶対温度 $T = 450\text{K}$)に至るまで十分な磁気性能を発揮できなければならないが、磁石材料の性能を特徴づける残留磁化 M_r と保磁力 H_c において後者の耐熱性が問題になりやすい。その一つの原因是、 $[M_r(T), H_c(T)]$ に対応する物性値 $[M_s(T), K_{u1}(T)]$ (M_s は自発磁化、 K_{u1} は一軸磁気異方性エネルギー)において、 $K_{u1}(T)$ の耐熱性が $M_s(T)$ より弱いことにあり、両者の有限温度スケール関係 $K_{u1}/K_{u1}(0) \propto [M_s(T)/M_s(0)]^\alpha$ が1イオン起源の磁気異方性に対して議論されてきた¹⁾。ここでスケール指数は $\alpha = l(l+1)/2$ とかかれ、 l は結晶場の局所的な対称性(正方晶で $l=2$ 、六方晶で $l=3$ 、立方晶で $l=4$)から決まる。希土類永久磁石は金属材料でもあることから、絶縁体的な1イオン磁気異方性の議論の妥当性は慎重に吟味されなければならない。実際、磁気記録媒体のための金属磁性材料FePtにおいては $\alpha \sim 2.1$ であり²⁾、1イオン描像の適用範囲外の磁気異方性発現メカニズムが示唆される。キュリー温度近辺に至るまで磁気異方性の耐熱性を出すためには α ができるだけ小さいことが望ましい。今日の希土類永久磁石の主流をなすNd-Fe合金においてFePt類似の耐熱磁気異方性を実現する方向性を検討する。

2 結果および考察

有限温度物性値において最強磁石化合物 $\text{Nd}_2\text{Fe}_{14}\text{B}$ を超えた $\text{NdFe}_{12}\text{N}_x$ ³⁻⁵⁾ に対し、第一原理に基づいてたてたスピン模型から有限温度磁化 $M(T)$ と異方性磁場 $H_a(T)$ を計算した⁶⁾。一軸磁気異方性エネルギーを $K_{u1}(T) \equiv H_a(T)M_s(T)/2$ の関係から見積もり磁化と磁気異方性のスケール特性を解析すると図1(a)のようになる(J_{TT} は第一原理計算から与えられる鉄原子間の交換結合⁶⁾、 J_{RT} は $4f\text{-}3d$ 交換結合⁷⁾、 K_{Nd} は Nd の結晶場係数の第一原理計算⁸⁾から与えられる一軸磁気異方性エネルギー)。交換定数をモデルパラメータとして有限温度磁気物性値の傾向を調べた結果、交換結合の強さに応じて磁化と磁気異方性エネルギーのスケール指数が変化することがわかる。モデルパラメータに依存するスケール指数の傾向をまとめると図1(b)のようになる。特に希土類・鉄間の交換結合が十分に強い場合、FePt類似の $K_{u1}(T) \sim M(T)^2$ 則が数値的に観測される。スケール指数の下がる傾向は、Fe-Fe交換結合が固定されているとしてNd-Fe交換結合を強くするか、あるいはNdの磁気異方性が固定されているとしてFe-Fe交換結合を強める方向に見られ、特に前者の影響が甚大である。いずれもNdの磁気異方性の1イオン性を弱める方向である。 $4f$ 電子の局在性を弱めて基底状態磁気異方性を若干犠牲にすることがあっても、 $4f$ 電子に若干の遍歴性を持たせて周辺の伝導電子との混成を促し、交換相互作用的な磁気異方性を出すことが高温特性改善につながると考えられる。

References

- 1) H. B. Callen and E. Callen, J. Phys. Chem. Solids. **27**, 1271 (1966).
- 2) S. Okamoto, N. Kikuchi, O. Kitakami, T. Miyazaki, Y. Shimada, and K. Fukamichi, Phys. Rev. B **66**, 024413 (2002).
- 3) T. Miyake, K. Terakura, Y. Harashima, H. Kino, and S. Ishibashi, J. Phys. Soc. Jpn. **83**, 043702 (2014).
- 4) Y. Hirayama, Y. K. Takahashi, S. Hirosawa, and K. Hono, Scr. Mater. **95**, 70 (2015).
- 5) Y. Hirayama, T. Miyake, and K. Hono, JOM **67**, 1344 (2015).
- 6) MM, H. Akai, Y. Harashima, S. Doi, T. Miyake, J. Appl. Phys. in press.
- 7) Ndの電子状態をopen coreとして扱い、Ndの5d電子とFeの3d電子の交換結合を第一原理から与えた上で、局在4fモーメントのスピン成分と5dバンドのスピン成分が十分に強く結合している(仮にfrozen 4f-5d近似と呼ぶ)として4f-3d交換結合を算出した。
- 8) Y. Harashima, K. Terakura, H. Kino, S. Ishibashi, and T. Miyake, JPS Conf. Proc. **5**, 011021 (2015).

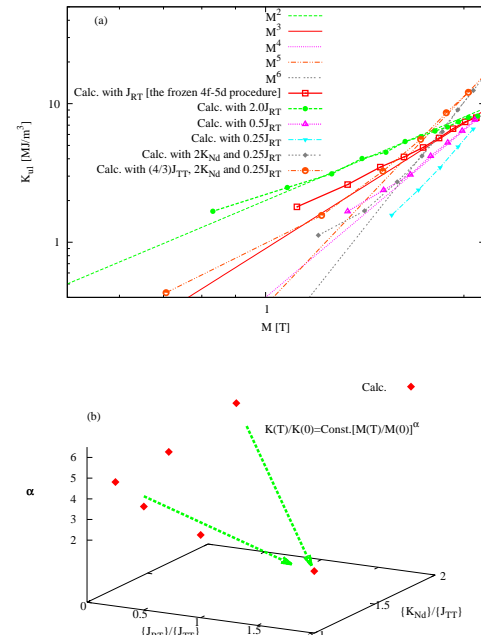


Fig. 1 Finite-temperature scaling of the magnetic anisotropy energy $K_{u1}(T)$ with respect to the magnetization $M(T)$ of NdFe_{12}N within a spin model. (a) Results with several input parameters. (b) Overview of the scaling exponent on a space of the model parameters. The arrows are guides for the eye.

Nd-Fe-B 磁石における磁化反転機構の解析

吉岡匠哉, 土浦宏紀

(東北大学大学院工学研究科, ESICMM)

Analysis of Magnetization Reversal Mechanism in Nd-Fe-B Magnets

Takuya Yoshioka, Hiroki Tsuchiura

(Tohoku University, ESICMM)

緒言

希土類磁石, 特に Nd-Fe-B 磁石の保磁力機構を解明することは, 工業的応用のみならず学術的見地からも極めて重要である。そのためには, 主相と粒界相の磁気的性質を微視的な立場から明らかにする必要がある。一方で, 応用上もっとも興味深い保磁力の評価を行うためには, 電子論的計算手法は現在のところ不十分であり, マイクロ磁気学シミュレーションの手法に頼ることになる。したがって, 現時点できりうる最前の理論的アプローチは, 微視的・電子論的計算から得られた情報を最大限取り入れたマイクロ磁気学シミュレーションモデルを構築し, それを用いて保磁力評価を行うことである。そこで我々は, 各イオンのもつ磁気モーメントをはじめ, Nd サイト, Fe サイトの局所的磁気異方性, Nd-Fe 間および Fe-Fe 間の交換相互作用といった情報を第一原理計算に基づき評価し, Nd₂Fe₁₄B 相を表現する有効スピンモデルを構築した。本講演では, このモデルを用いて Nd-Fe-B 磁石の有限温度における磁気異方性や保磁力を計算した結果について報告する。

計算手法

希土類永久磁石の結晶磁気異方性は, 主に希土類イオンの 4f 電子に働く結晶電場によってもたらされる。結晶電場を定めるのは 4f 電子の周囲にある電荷分布であり, これは第一原理計算を用いることにより正確に計算することが出来る。まず, 第一原理計算コード WIEN2k を用いて Nd₂Fe₁₄B の電子状態を解析し, 結晶電場ハミルトニアン H_{CEF} を構築する。次に, ハミルトニアンに基づく自由エネルギーから有限温度の磁気異方性定数を見積もる。最後に原子スケールの LLG 方程式に従って保磁力を計算する。ここで各イオン磁気モーメント, Fe 副格子の磁気異方性, 交換相互作用に関しては実験値を援用する。

結果

Nd₂Fe₁₄B における磁化反転プロセスを下図に示す。ここでは(001)表面に Nd イオンが露出している状況を想定している。本講演では, 実験に対応した界面をもつ微視的スピンモデルを構築し, マイクロ磁気学シミュレーションの結果から保磁力低下の原因について議論する。

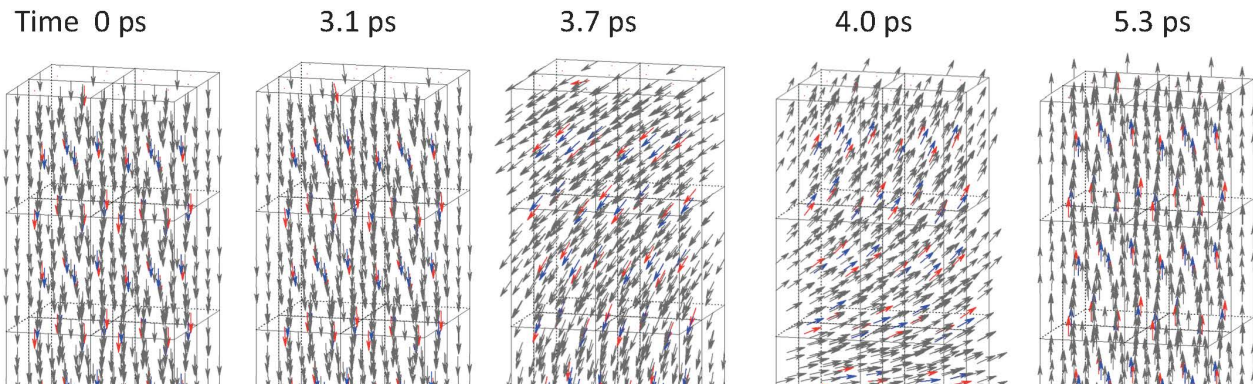


図 磁化反転プロセス

Analyses on magnetization reversal process of Nd-Fe-B hot-deformed magnets

S. Okamoto^{1,2}, T. Yomoita¹, L. Zhang¹, N. Kikuchi¹, O. Kitakami¹,
H. Sepehri-Amin², T. Ohkubo², K. Hono², T. Akiya³, K. Hioki³, and A. Hattori³
(¹Tohoku Univ., ²ESICMM-NIMS, ³Daido Steel)

The magnetization reversal process of a Nd-Fe-B magnet has been long a controversial issue since its discovery. Recently, the importance of this subject becomes more significant because of the growing demands of high performance permanent magnets for electric/hybrid vehicle and generator applications. Since a Nd-Fe-B magnet has a microstructure of the Nd₂Fe₁₄B main phase grain and the intergrain phase, it has been widely accepted that the grain boundary plays a crucial role for the magnetization reversal process. In Nd-Fe-B sintered magnets, however, the grain boundary direction is randomly distributed with respect to the *c*-axis of Nd₂Fe₁₄B phase. On the other hand, a Nd-Fe-B hot-deformed magnet has a microstructure of well aligned platelet Nd₂Fe₁₄B gran, and the grain boundary mostly exists along the directions of parallel and perpendicular to the *c*-axis of Nd₂Fe₁₄B phase. Thus, a Nd-Fe-B hot-deformed magnet is expected to be a model magnet for the analysis of the magnetization reversal process. In this talk, we discuss the magnetization reversal process of the Nd-Fe-B hot-deformed magnets through the magnetic viscosity [1] and the first-order reversal curve (FORC) analyses [2].

The samples used in this study are the Nd-Fe-B hot-deformed magnets with and without the Nd-Cu eutectic alloy grain boundary diffusion process [3]. The former and latter are referred as GBD and HD, respectively. The coercivity H_c of these two samples are quite different, i.e. 2.2 T for GBD and 1.1 T for HD at ambient temperature. Under finite temperature, the magnetization reversal takes place through the thermal activation process against the energy barrier $E_b(H)$. $E_b(H)$ is usually expressed as $E_b(H) = E_0(1 - H/H_0)^n$, where H is the magnetic field, E_0 the energy barrier height at $H = 0$, n the constant depending on the magnetization reversal mode; $n = 1$ for domain wall pinning and $n = 1.5 \sim 2$ for nucleation or coherent rotation. Recently we proposed the method to determine these energy barrier parameters from the magnetic viscosity measurement [1]. Fig. 1 shows the value of n for HD and GBD magnets as a function of temperature. Surprisingly, the value of n almost keeps to be 1 irrespective of temperature and samples whereas H_c varies significantly with temperature and samples. This fact indicates that the domain wall pinning is the major magnetization reversal process at $H \approx H_c$. Fig. 2 shows the FORC diagrams of HD and GBD samples. For this experiment, the samples are shaped into long rods of 3*0.5*0.5 mm³ in order to reduce the demagnetization factor N_z . Both the FORC diagrams of HD and GBD exhibit simple Gaussian patterns with narrow distributions. From these results, we may conclude that the effect of local demagnetization field which has been frequently discussed is negligibly small, and the coercivity distributions are also very small. This work was partially supported by ESICMM

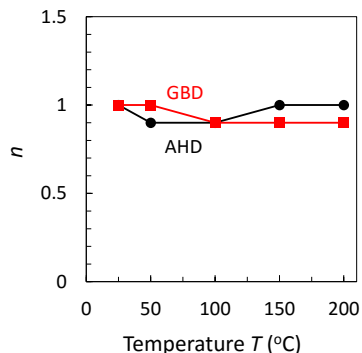


Fig. 1 Power index n of energy barrier function as a function of temperature.

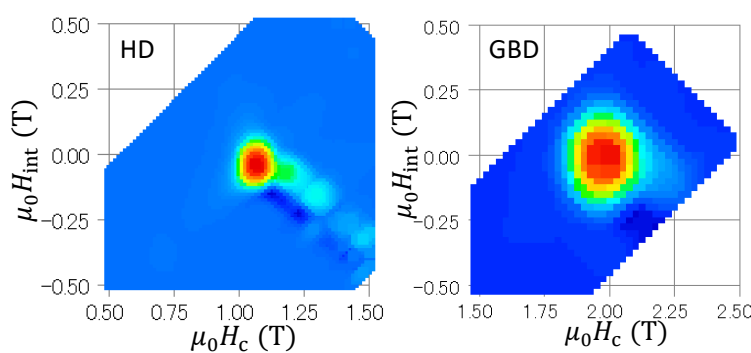


Fig. 2 FORC diagrams of HD and GBD samples at ambient temperature.

References

- [1] S. Okamoto et al., J. Appl. Phys. **118**, 223903 (2015), [2] T. Yomoita et al., submitted to proceedings of PEPM2016,
- [3] T. Akiya et al., Scr. Mater. **81**, 48 (2014).

確率的 Landau-Lifshitz-Gilbert 方程式による $\text{Nd}_2\text{Fe}_{14}\text{B}$ 磁石の原子論的モデルにおける磁化反転ダイナミクス

西野正理¹、宮下精二²

(¹物材機構、²東大院理)

Dynamics of magnetization reversal in atomistic models of $\text{Nd}_2\text{Fe}_{14}\text{B}$ magnets by the Stochastic

Landau-Lifshitz-Gilbert equation

Masamichi Nishino¹ and Seiji Miyashita²

(¹NIMS, ²Univ. of Tokyo)

イントロダクション

Landau-Lifshitz-Gilbert(LLG)方程式は、磁化ダイナミクスを記述する基礎方程式である。マイクロマグネティクスにおいては、しばしば連続体モデルによる LLG シミュレーションが行われるが、我々は結晶格子上の各原子がもつ磁気モーメントを考慮して磁気的相互作用をモデル化する原子論的な立場からの LLG 法によるダイナミクスを調べている[1,2]。この方法の長所は微視的に磁化反転ダイナミクスを調べることが出来る点にある。一方、連続体で有利な大きな系の取り扱いには困難が生じる。LLG 方程式はそのままでは温度による効果を記述できない。我々は LLG 方程式に stochastic noise を導入することにより、不均一磁化系への温度効果を正確に取り込んだ方法論を得て[1]、磁化反転における核生成や depinning 機構などについて研究を進めている。ここでは、この Stochastic Landau-Lifshitz-Gilbert (SLLG)法による不均一磁化系のダイナミクスへの適用と $\text{Nd}_2\text{Fe}_{14}\text{B}$ 磁石 系のモデル系へ適用して得られた磁化の動的特性について報告する。

磁化ダイナミクス

熱平衡を実現するダイナミクスにおいて、SLLG 方程式の緩和定数とノイズの大きさの選び方に任意性があり、揺動散逸関係を満たす限り平衡状態に漸近するが、その選択によってダイナミクスには一般に相違が現われることが分かっている[1]。この事に注意して、 $\text{Nd}-\text{Fe}-\text{B}$ 系の原子論的スピニモデルに対して、SLLG 法による有限温度のダイナミクシミュレーションを行った。赤井らによる第一原理計算から見積もったパラメータを用いることで、 $\text{Nd}-\text{Fe}-\text{B}$ 系固有の磁化反転や自発磁化などの物性に関して、定性的のみならず定量的な解析が可能となった。まず、SLLG 法での定常状態は熱平衡状態であるが、この手法を用いて熱平衡状態のシミュレーションを行い、モンテカルロ計算で得た値と比べて一致することを確認した。そして、実験値に近い転移温度の見積もりや磁気再配列転移の特徴を再現することが出来た。また、 $\text{Nd}-\text{Fe}-\text{B}$ の一辺 10 ユニットセル程度の境界条件の異なるいくつかの系に対して、磁化反転ダイナミクスのシミュレーションを行った。その結果、Nd サイトの磁化反転がしやすい事や、境界条件により反転の様子が変わることなどが分かった(図 1)。またドメインウォール幅は 2~3 ユニットセル程度の大きさ(400K)を持つことや (図 2)、核生成的な反転過程が現われる事が観察された。また、ドメインは必ずしも c 軸方向に成長しやすいのではなく、条件により異なる成長の可能性が観察された。

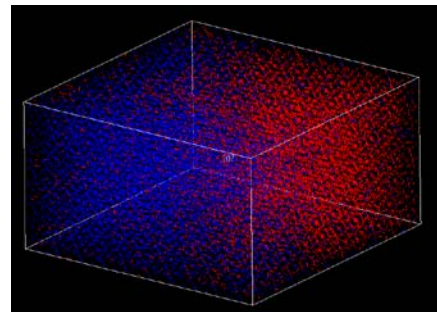


図 1 磁化反転の様子
(open boundary)

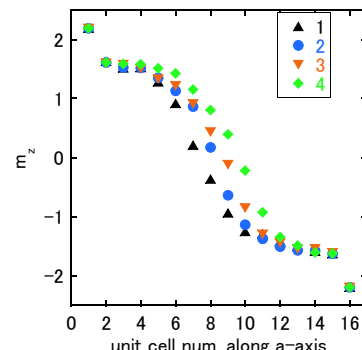


図 2 ドメインウォール幅

参考文献

- 1) M. Nishino and S. Miyashita, Phys. Rev. B. 91, 134411 (2015).
- 2) S. Mohakud, S. Andraus, M. Nishino, A. Sakuma, S. Miyashita, arXiv:1602.03285

Influence of microchemistry and interface structure of cell boundary phase on the coercivity of $\text{Sm}(\text{Co}_{0.78}\text{Fe}_{0.10}\text{Cu}_{0.09}\text{Zr}_{0.03})_{7.19}$ sintered magnets

H. Sepehri-Amin¹, J. Thielsch², T. Ohkubo¹, J. Fischbacher³, T. Schrefl³, O. Gutfleisch⁴, and K. Hono¹

¹National Institute for Materials Science, Tsukuba 305-0047, Japan

²IFW Dresden, Institute for Metallic Materials, P.O. Box 270116, D-01171 Dresden, Germany

³Center for Integrated Sensor Systems, Danube University Krems, Austria

⁴Materialwissenschaft, Technische Universität Darmstadt, D-64287 Darmstadt, Germany

Excellent hard magnetic properties of $\text{Sm}_2\text{Co}_{17}$ -type sintered magnets at elevated temperature make them the only choice for the applications above 300°C. However, the coercivity of $\text{Sm}_2\text{Co}_{17}$ -type permanent magnets strongly depends on the cooling rate from aging temperature of ~850°C; No coercivity for rapidly quenched sample while the coercivity is enhanced to ~2.0 T after slow cooling [1]. This has been correlated to the Cu content and its distribution in the cell boundary phase [2]. Questions raise here; does just small increase of Cu in the cell boundary phase substantially enhances coercivity or are there other microstructural features influencing the coercivity of $\text{Sm}_2\text{Co}_{17}$ -type permanent magnets? In this work, we have revisited the microstructure of $\text{Sm}_2\text{Co}_{17}$ -type sintered magnets with different coercivity levels and discussed the coercivity mechanism by employing finite element micromagnetic simulations to answer to these open questions.

Commercial $\text{Sm}(\text{Co}_{0.784}\text{Fe}_{0.100}\text{Cu}_{0.088}\text{Zr}_{0.028})_{7.19}$ sintered magnets with two different heat treatment conditions, one quenched rapidly and the other slowly cooled from 850°C were studied. The magnetic properties of the samples were measured using a SQUID-VSM. Microstructure of the samples were analyzed using SEM/FIB (Carl Zeiss 1540EsB), TEM (Titan G2 80-200) and 3DAP. Influence of the microchemistry of the cell boundary phase to its pinning strength was studied using micromagnetic simulations.

The sample slowly cooled down from 850°C showed the high coercivity of 2.6 T, while coercivity of the quenched sample was only 0.14 T. Figure 1 (a) and (b) show high resolution STEM-HAADF images obtained from the quenched and slowly cooled samples respectively. $\text{Sm}_2\text{Co}_{17}$ matrix phase, SmCo_5 cell boundary phase, and Z-phase are observed in the microstructure. Unlike the quenched sample, $\text{SmCo}_5/\text{Sm}_2\text{Co}_{17}$ interface is sharp and smooth in the slowly cooled sample. Figure 1 (c) and (d) show 3D atom maps of Sm and Cu and their composition profiles obtained from the two different cell boundaries of the quenched and slowly cooled samples. Enrichment of 8.6 at. % of Cu and 7.7 at. % Fe was found in the cell boundary of the quenched sample while the SmCo_5 cell boundary phase of slowly cooled down sample contains 15.4 at. % of Cu and 3.0 at. % Fe. In addition, the distribution of Cu broader than that of Sm was found in the cell boundary of the quenched sample. Micromagnetic simulations showed that the enrichment of Fe in the cell boundary and the broad distribution of Cu results in a smaller gradient of K_1 through the 2:17/1:5 interface, which decreases the pinning strength of the cell boundary phase. This explains the low coercivity in the quenched sample.

[1] D. Goll, et al. Appl. Phys. Letters 76 (2000) 1054-1056. [2] X. Y. Xiong, et al. Acta Mater. 52 (2004) 737-748.

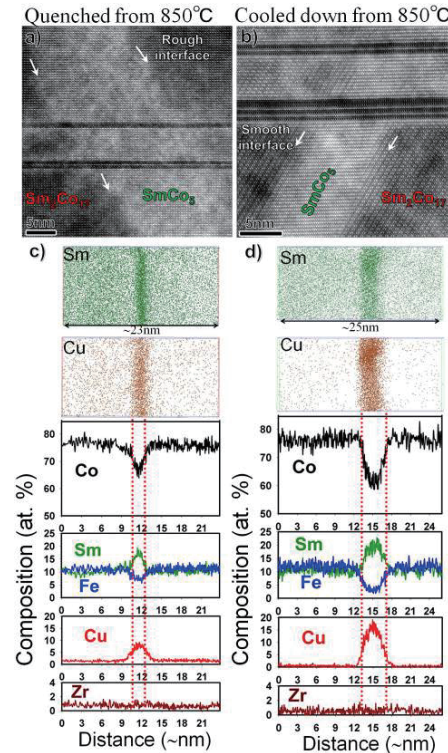


Fig. 1. (a) and (b) STEM-HAADF image and (c) and (d) 3DAP atom maps of Sm and Cu and calculated composition profile obtained from the $\text{Sm}_2\text{Co}_{17}$ -type magnets quenched and slowly cooled down from aging temperature of 850°C.

ネオジムボンド磁石の結晶粒表層の劣化と粒界相が磁気特性に及ぼす影響

赤城文子、酒井佑輔、本藏義信*

(工学院大、*マグネデザイン)

Effects of deterioration of grain surface-layer and grain boundary on magnetic property for neodymium permanent magnet

F. Akagi, Y. Sakai, Y. Honkura*

(Kogakuin Univ., *Magnedesign)

はじめに

近年、環境への配慮や資源の枯渇問題から、より効率の高いモータの需要が高まっている。ネオジムボンド磁石は形状自由度が高く、小型化・軽量化に優れているが、角形性及び保磁力が焼結磁石より劣る¹⁾。前回の報告では、1個の結晶粒を小さなセルに分割して MH ループを求め、それが、複数個集まったものとして相加平均を求め、結晶粒表層の劣化（磁気異方性の劣化）や主相の磁気異方性の分散が保磁力及び角形性を劣化させることを示した²⁾。しかし、結晶粒間の交換相互作用や静磁界は考慮していなかった。本研究では、これらを考慮し、結晶粒表層の劣化と粒界相が MH ループに及ぼす影響を検討した結果を報告する。

計算方法

計算は磁界シミュレータ EXAMAG を用いた³⁾。本プログラムでは、有限要素法を用いて Landau-Lifshitz-Gilbert 方程式 (LLG 方程式) を解き、媒体の磁化を求める。Fig. 1 に計算に用いた永久磁石のモデルを示す。1つの結晶粒は $40 \times 40 \times 40 \text{ nm}^3$ とし、結晶粒界幅は 2 nm、結晶粒表層の劣化層の幅は 2 nm とした。結晶粒の飽和磁化は 1.61 T、粒界相は 0.805 T とした。交換結合定数は、結晶粒及び結晶粒と粒界相間が $1.00 \times 10^{-11} [\text{J/m}]$ 、粒界相は $6.25 \times 10^{-12} [\text{J/m}]$ とした。結晶粒の主相の異方性磁界は 6077 [kA/m] とし、表層劣化層の異方性磁界は主相の 10% とした。また、粒界相内は軟磁性として、異方性磁界は 1 [kA/m] とした。MH ループは容易軸角度を Fig. 1 の +y 軸方向から +x 軸方向に 10° ずつ増加させて求めた。

計算結果

Fig. 2 は結晶粒表層の劣化の有無と、粒界相が非磁性か軟磁性かの違いによる保磁力の容易軸角度依存性の比較結果である。図より、表層の劣化が無い場合、粒界相が非磁性である理想的な場合に比べ、粒界相が軟磁性であれば、保磁力は劣化するが、実測⁵⁾に比べると保磁力は非常に高く Stoner-Wholfarth 型の容易軸角度依存性を示す⁴⁾。一方、表層に劣化層がある場合は、粒界相の磁性、非磁性に対する保磁力の差は小さい。更に、両者ともに、保磁力は実測に近い値となる。即ち、保磁力は表層の劣化層に大きく依存する。

参考文献

- 1) Y. Honkura, Proceeding of the 19th International Workshop on Rare Earth Permanent Magnets and Their Application, Beijing, China, p. 231, 2006.
- 2) F. Akagi and Y. Honkura, The 39th Annual Conference on MAGNETICS in Japan, Symposium 09A-1, 2015.
- 3) Fujitsu Japan - 富士通 <http://pr.fujitsu.com/jp/news/2013/12/10.html>.
- 4) 上原裕二、第3回岩崎コンファレンス、2014.
- 5) <http://www.magfine.net/magfine/images/MAGFINE%20CATALOG%20A4%20ENG%20BACK.pdf>.

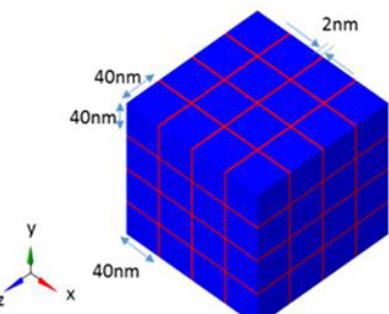


Fig. 1 Permanent magnet model.

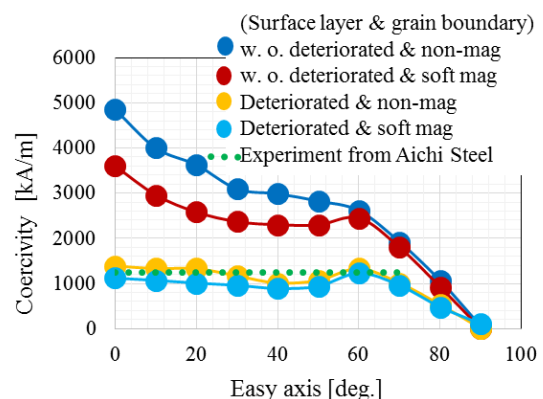


Fig. 2 Easy axis dependence of coercivity.